



# Impact of climate change and land cover dynamics on nitrate transport to surface waters

Hulya Boyacioglu · Mert Can Gunacti ·  
Filiz Barbaros · Ali Gul · Gulay Onuslu Gul ·  
Tugba Ozturk · M. Levent Kurnaz

Received: 6 October 2023 / Accepted: 29 January 2024  
© The Author(s), under exclusive licence to Springer Nature Switzerland AG 2024

**Abstract** The study investigated the impact of climate and land cover change on water quality. The novel contribution of the study was to investigate the individual and combined impacts of climate and land cover change on water quality with high spatial and temporal resolution in a basin in Turkey. The global circulation model MPI-ESM-MR was dynamically downscaled to 10-km resolution under the RCP8.5 emission scenario. The Soil and Water Assessment Tool (SWAT) was used to model stream flow and nitrate loads. The land cover model outputs that were produced by the Land Change Modeler (LCM) were used for these simulation studies. Results revealed

that decreasing precipitation intensity driven by climate change could significantly reduce nitrate transport to surface waters. In the 2075–2100 period, nitrate-nitrogen ( $\text{NO}_3\text{-N}$ ) loads transported to surface water decreased by more than 75%. Furthermore, the transition predominantly from forestry to pastoral farming systems increased loads by about 6%. The study results indicated that fine-resolution land use and climate data lead to better model performance. Environmental managers can also benefit greatly from the LCM-based forecast of land use changes and the SWAT model's attribution of changes in water quality to land use changes.

---

**Supplementary Information** The online version contains supplementary material available at <https://doi.org/10.1007/s10661-024-12402-x>.

---

H. Boyacioglu (✉)  
Department of Environmental Engineering, Dokuz Eylul University, Izmir, Turkey  
e-mail: hulya.boyacioglu@deu.edu.tr

M. C. Gunacti · F. Barbaros · A. Gul · G. O. Gul  
Department of Civil Engineering, Dokuz Eylul University, Izmir, Turkey

T. Ozturk  
Faculty of Engineering and Natural Sciences, Department of Physics, Isik University, Istanbul, Turkey

M. L. Kurnaz  
Center for Climate Change and Policy Studies, Bogazici University, Istanbul, Turkey

**Keywords** Climate change · SWAT model · Water quality modeling

## Introduction

In parallel with changing climatic conditions, anthropogenic activities and related land cover changes have had adverse effects on water resources in the last few decades. Water resource management becomes a much more crucial topic under the impacts of climate and land cover change when it comes to mitigating their economic, social, and environmental effects. Extreme meteorological conditions that are driven by climate change cause flooding and severe droughts (Mustafa et al., 2019; Szpakowski & Szydlowski, 2018). Thus, changes in streamflow characteristics

affect the transport and dilution of pollutants (Rostami et al., 2018). Increasing the use of agricultural fertilizers and urban pollutants has a major effect on water quality in the region (Choi et al., 2021; Mahmoodi et al., 2021; Whitehead et al., 2009; Yang et al., 2018). The spatiotemporal variation in land use and land cover (LULC) has a direct impact on both the quantity and quality of runoff. This can be supported by several factors: (1) urbanization, (2) deforestation, (3) agricultural practices, and (4) climate change. Overall, the relationship between spatiotemporal changes in LULC and runoff quantity and quality is well documented in scientific literature and supported by empirical evidence from various regions around the world (Mustafa & Szydlowski, 2020; Hashim et al., 2022; Bai et al., 2019; Delia et al., 2021; Zhu et al., 2022 and Zango et al., 2022). One of the most comprehensive models that can simulate both the quantity and quality of surface water and groundwater is the “Soil Water Assessment Tool (SWAT)” which was developed by the USDA Agricultural Research Service (USDA-ARS). The model has been used by researchers to study the hydrological cycle and water quality under climate and land cover change (Abbaspour, 2015). Many studies on water quality management by SWAT were carried out for nutrients in the literature (Mehdi et al., 2015; Sholichin & Prayogo, 2021). The results of several studies concluded that changes in the hydrological cycle could directly affect the transport of various water pollutants, including but not limited to nitrate-nitrogen ( $\text{NO}_3\text{-N}$ ) and phosphate phosphorus ( $\text{PO}_4\text{-P}$ ) in the environment (Hosseini et al., 2017; Yang et al., 2018). According to study findings conducted by Khadka et al. (2023), Amiri et al. (2023), and Serpa et al. (2017), the SWAT model may generate reasonably accurate hydrologic and water quality predictions with regard to climate change and future land cover impacts when it is properly calibrated.

The studies in the literature mostly did not use a dynamic land use modeling approach to evaluate the impact of land use changes on water quality. The novel contribution of the study was to investigate the individual and combined impacts of climate and land cover change on water quality with high spatial and temporal resolution. The impact of climate and land cover change on water quality based on land cover estimations created by artificial neural network (ANN)-oriented approaches and climate

predictions with high spatial and temporal resolution in the Kucuk Menderes River Basin (KMRB), Turkey, was investigated. The SWAT was used to evaluate the impact of changes on surface water nitrate content under climate and land use change scenarios. Although it was used in hydrological modeling (e.g., Anand et al., 2018; Gashaw et al., 2018; Mekonnen & Manderso, 2023), this will be one of the pioneering studies in the literature that the SWAT model was used to determine impacts on water quality under future land use scenarios that were predicted using the ANN approach. Moreover, individual and combined impacts of climate and land cover change on water quality with high spatial and temporal resolution were investigated.

## Materials and methods

In the study, SWAT was used to simulate streamflow and nitrate loading under different climate and land cover scenarios in KMRB, Turkey. Detailed information on the study area and climate, land use, hydrology and water quality modeling is given below.

### Study area

The KMRB is located in western Turkey and has a 3454 km<sup>2</sup> catchment area (Fig. 1). The population of the basin was about 562,000 in 2022 (TURKSTAT, 2023). Land cover distribution in the region is as follows: agricultural land (AGRR\_W, AGRR\_nonW and OLIV) (58%), forest and semi-natural areas (FRST and PAST) (39%), artificial surfaces (URML, UTRN and BARR) (2.66%), wetlands (0.23%), and water bodies (WATR) (0.22%) (Figure S1). In the basin, the usual traits of the Mediterranean climate are predominant. It has a dry and hot summer and a cool and rainy winter. Since there are intensive agricultural activities, the deficit of surface water is one of the main issues in the region. As a result, agricultural communities in the basin seek to fulfill their irrigation water needs by exploiting groundwater resources with an increasing demand, which is also declining (Gunacti et al., 2022; MoAF, 2019).

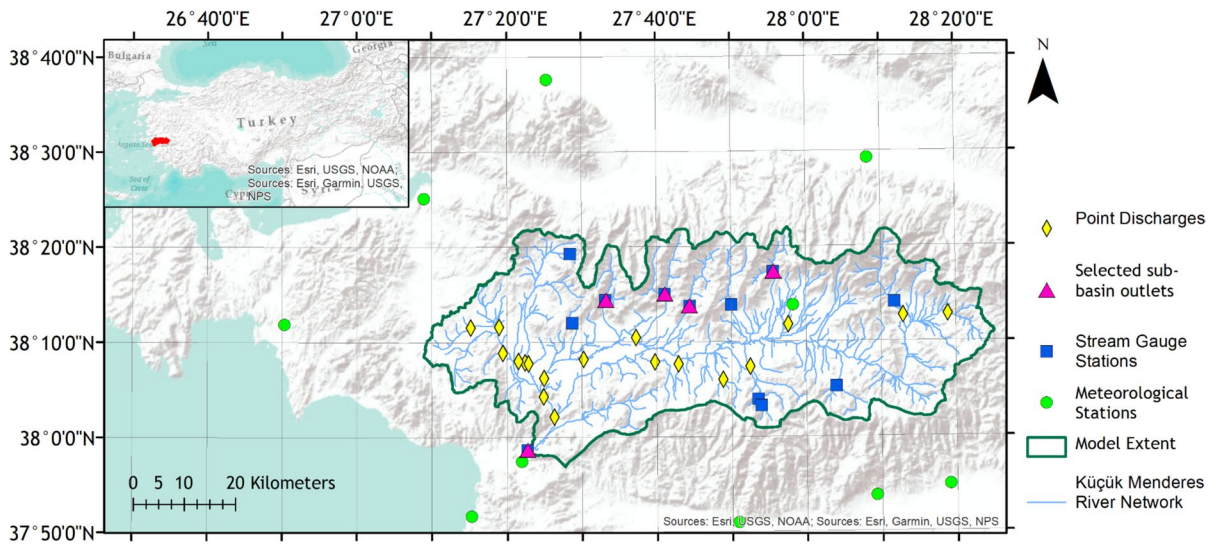


**Fig. 1** Study area

**Datasets**

**Meteorological and hydrological data** In the study, required meteorological and hydrological data were obtained on a daily basis from the Turkish State Meteorological Service (MGM) and State Hydraulic Works (DSI). Data from the 12 streamflow gauging and 10 meteorological observation stations were used in the modeling study. The locations of the stations are depicted in Fig. 1. The solar radiation data that were not observed by local authorities were obtained from the SWAT model global database (Climate Forecast System Reanalysis- CFSR, data range 1979–2014) (Saha et al., 2014). Moreover, in cases of discontinuity in meteorological data sets, the meteorological data generator table (WGEN) of the SWAT database was used to generate continuous data.

**Geophysical data** The Digital Elevation Model (DEM) is one of the main materials in this study and contributes to both land cover change and hydrological models. DEM for the basin at 10-m resolution was developed for the study using 1:5000 maps. Using DEM and Coordination of Information on the Environment (CORINE) data sets, the remaining set of inputs for land cover change modeling were primarily produced via ArcGIS software tools (Gunacti et al., 2022).

**Land cover data** CORINE land cover data was used in the land cover change modeling study (Gunacti et al., 2022). Data for the study area for the years 1990, 2000, 2006, 2012, and 2018 were compiled separately. The CORINE and SWAT database land cover classes were matched and reclassified down to nine distinct classes for the model (Gunacti et al., 2022) (see Table S1).

The classification of the cover types included level 1, 2, and 3 classification genres of CORINE as the focus of the study requires.

- WATR represents “Water Bodies.”
- BARR, FRST, PAST, and URML, represent “Mine, dump and construction sites,” “Forest,” “Shrub and/or herbaceous vegetation associations,” and “Urban fabric,” respectively.
- AGRR\_W, AGRR\_nonW, OLIV, and UTRN represents “Permanently irrigated land,” “Non-irrigated arable land,” “Olive groves,” and “Road and rail networks and associated land,” respectively.

Moreover, soil data were compiled from different databases, which are global open access or government/institutional sources. Multi-spectrum Landsat satellite images with a terrestrial resolution of 30 m were compiled from the United States Geological

Survey (USGS) – Earth Explorer database (EarthExplorer, 2019) to produce the albedo layer. Soil profile data for 250 m was obtained from the SoilGrids database (Soilgrids, 2019).

**Water quality and pollutant source data** In the study, basin hydrology was simulated using the streamflow discharges observed at the gauging station located at the basin outlet. The calibration and validation periods were determined considering the availability of simultaneously observed meteorological and hydrometric data. For the calibration and validation processes of the water quality model, the required data (observed surface water quality and discharge data) for the basin outlet monitoring station were provided by local authorities. Details on the calibration and validation of hydrologic and water quality models are provided under the following sections titled “Hydrologic modeling” and “Water quality modeling.” As is seen in Table S2, the frequency of the observed water quality records was generally on a monthly and bimonthly bases. Wastewater discharge loads from point sources (domestic and industrial) were estimated either based on the water quality characteristics or calculated using discharge records. Furthermore, fertilizer consumption records were provided by either local authorities or farmer associations, and the amount of fertilizer applied was given to the model as an input.

#### Climate modeling

In the study, the regional climate model RegCM (RegCM4.4) was used to produce high-resolution regional climate simulations. The RegCM has been used in regional climate change studies throughout the world for the last two decades (Agacayak et al., 2015; Oğuz & Akın, 2018). RegCM is a hydrostatic regional climate model and developed by the Abdus Salam International Center for Theoretical Physics (ICTP). The dynamic structure of the model was developed from the MM5 (the Mesoscale Model 5) model of the Pennsylvania State University National Research Center (Solaimani et al., 2023). BATS1E (Biosphere–Atmosphere Transfer Scheme) has been used for surface-related processes, and Community Land Model (CLM) version 3.5 is given as an option to be included in the dynamic structure of the model. Radiative transfer is formed using the

NCAR Community Climate Model, version CCM3 radiation package, whereas solar radiation transfer is modeled by the  $\delta$ -Eddington approximation (Kiehl et al., 1996). The regional climate model uses three parameters, such as partial cloudiness, the liquid water content of the cloud, and the effective droplet radius, to simulate the cloud radiation. The planetary boundary layer (PBL scheme) is used in the model. The convective precipitation patterns of the model are calculated by choosing one of three schemes: the modified-Kuo scheme, the Grell scheme, and the MIT-Emanuel scheme (Koulov & Zhelezov, 2016). The Grell scheme was employed with the Fritsch-Chappell-type closure in simulating the convective rainfall for present and future projections (Demiroglu et al., 2015).

The RegCM4.4 version was used to downscale the global climate data to 10-km resolution by the double nesting method in the presented study. The global circulation model MPI-ESM-MR of the Max Planck Institute for Meteorology was dynamically downscaled to 10-km resolution under RCP8.5 emission scenarios. Future changes in climate variables were calculated for the future period of 2025–2100 compared to the reference period of 1971–2000.

In the study, the MPI-ESM-MR global climate model was selected to downscale RegCM4.4 since it has a medium equilibrium climate sensitivity within the CMIP5 ensemble; on the other hand, its performance over most CORDEX-CORE (Coordinated Regional Climate Downscaling Experiment–Coordinated Output for Regional Evaluation) domains is reasonably good (Ozturk, 2023). Even though the ensemble approach, based on the ensemble mean of multi-model results, has been an approved technique in the regional modeling community, running the regional climate model with more than one driving field in high resolution is expensive. For this reason, we picked the most reasonable global climate model to downscale to provide data for this impact study. Model performance includes a simple qualitative discussion of the comparison between the model and observational datasets of precipitation given by Ozturk et al. (2018). According to their results, RegCM outputs driven by MPI-ESM-MR show better agreement than the results of RegCM driven by the HadGEM2-ES global model concerning the observational dataset over the MENA (Middle East and North Africa) region, including Turkey. The ability of

the model to reproduce observed conditions was reasonable (Ozturk et al., 2018).

### Land cover change modeling

Land cover change modeling was conducted using the LCM, a software tool called TerrSet, developed by Clark Labs (Gunacti et al., 2022). The LCM tool uses the multi-layer perceptron (MLP) and Markov cellular automata (MCA) techniques to forecast future land cover classes (Ansari & Golabi, 2019). The model's general process includes spatial change analysis for historical land cover data, defining the relevance of the driver variables with the model data, developing a transition sub-model (MLP-MCA), validating the sub-model, and making future predictions (Gunacti et al., 2022). The latest CORINE land cover maps were utilized to represent the historical (the years 2006 and 2012) and validation (the year 2018) data. As for the driver variables of the transition sub-model, DEM, slope, distance to urban areas, rivers, roads, urban development areas, and water bodies were included since they highly influence the land cover change (Figure S2) (Khoi & Murayama, 2010; Kim et al., 2014). For the validation of the model, ROC analysis was carried out for each land cover class. In Figure S3, true-positive and false-positive ROC curves were given for each land cover class. According to the ROC curve, high accuracy is indicated by the fact that true-positive values tend to be closer to true-positive values than false-positive values. Future land cover maps up to the year 2100 were produced using the validated model (Gunacti et al., 2022). The methodology of the land cover modeling study is briefly summarized below.

The MLP approach, which is commonly used in land cover change modeling methods, is divided into three layers: input, output, and hidden. MLP establishes the weights between the input and output layers by training the neural network based on mathematical correlations (Tu, 1996). MLP randomly selects multiple pixels for training and assessment according to the following criteria: (a) one-half of the pixels switched from one land cover class to the examined sub-model land cover class/classes, whereas the other half did not; (b) the pixels are then randomly allocated into two groups, one for training and one for validation, with each group having half of the pixels (Gunacti et al., 2022).

The training pixels are used to train the MLP and compute the land cover change between historical land cover data, while the validation group is used to assess the training model's ability to properly forecast the persistence of land cover classes or their transition. The transition potentials obtained from this training and validation procedure are then incorporated into a transition matrix, which is used to predict the land cover maps for future periods (Gunacti et al., 2022).

For spatial and temporal dynamic modeling, in TerrSet, the combination of MLP with the CA-Markov method is established, and then, the land cover change model is validated using the relative operating characteristic (ROC) curve, which is used to assess the accuracy or performance of the land cover change model. (Gunacti et al., 2022; Yariyan et al., 2020).

Estimated land use maps for the years 2050, 2075, and 2100 are seen in Figure S4.

### Hydrologic modeling

In the initial part of the nutrient modeling study, to estimate nitrogen fluxes in the study area, hydrologic simulation was performed. Monthly discharge at the outlet streamflow gauging station was simulated using SWAT. Input variables needed in SWAT modeling studies can be classified as (a) physical inputs and (b) meteorological inputs. The physical inputs consist of a representable DEM, a detailed soil map, and a land cover map. The meteorological inputs are maximum and minimum temperatures, solar radiation, precipitation, wind speed, and relative humidity, representing the investigated area.

The SWAT model operates the water balance on the scale of hydrologic response units (HRUs), which are called the smallest watershed units of a SWAT model and contain similar land cover and soil-type combinations within the sub-basin (Arnold et al., 2012).

In the study, the KMRB was discretized into 50 sub-basins, which were generated based on dominant land cover, soil, and slope. Monthly discharge at the outlet streamflow gauging station was calibrated and validated for the period 2000–2012. This period was determined based on the availability and quality of the data. Calibration and verification processes were performed using the calibration algorithm (SUFI-2) in the SWAT-CUP utility.

## Water quality modeling

The amount of nitrate transported (monthly) from the basin into the river was simulated using the SWAT model. Similar to the hydrologic modeling, sensitivity analysis, calibration, and validation processes were performed for the basin outlet streamflow gauging station using SWAT-CUP. Sensitivity analysis was applied to 12 parameters commonly used for nitrate-nitrogen calibration by evaluating the basin conditions and examining the literature. Sensitivity analysis in SWAT-CUP was performed by two methods:

- Global sensitivity analysis
- One-at-a-time sensitivity analysis

### Water quality modeling examination under scenarios

The impact of climate and land cover change on water quality was examined. In this study, the 2025–2050 period represented the “near-future” and 2050–2075 “mid-future” and 2075–2100 “far-future” accordingly. Model scenarios and data requirements for each scenario are given in Table 1.

In the study, the spatial differentiation of surface water nitrate loads under different scenarios was also examined. Monthly  $\text{NO}_3\text{-N}$  loads estimated at 50 sub-basin outlet points were evaluated to investigate spatial differentiation under climate and land cover change scenarios for each future period (near-, mid-, and far-future) individually. Accordingly, the

spatial distribution was mapped by considering the 90th percentile of the data set representing each time period.

The SWAT model was run under the reference period’s climatic conditions by changing only the land cover maps to estimate the impact of land cover change on water quality. In this context, estimated land cover maps for the years 2035 (for the near-future period), 2065, and 2085 (for the mid- and far-future periods) were used to represent the scenario periods.

In order to investigate the impact of climate change on water quality in each sub-basin, the SWAT model was run using estimated climate data. It was assumed that there was no change in land cover, and therefore, the 1990 CORINE land cover map was used to represent reference and future period land cover conditions.

The superposed impact of climate and land cover change on water quality was also evaluated. The model was run for:

- Near-future period, using land cover map estimated for the year 2035 and 2025–2050 climate estimations
- Mid-future period, using land cover map estimated for the year 2065 and 2050–2075 climate estimations
- Far-future period, using land cover map estimated for the year 2085 and 2075–2100 period climate estimations

**Table 1** Model scenarios and data requirement

The objective of the scenario	Data requirement			Reference period 1985–2009 Input data
	Near-future 2025–2050	Mid-future 2050–2075	Far-future 2075–2100	
Investigation of the impact of climate change	2025–2100 period climate estimations-model results Land cover map 1990-Corine			Observed meteorological and discharge data Land cover map 1990-Corine
Investigation of the impact of land use change	Land cover map for the year 2035 1985–2009 period observed discharged data	Land cover map for the year 2065	Land cover map for the year 2085	
Investigation of the combined impact of climate and land use change	2025–2100 period climate estimations-model results Land cover map for the year 2035	Land cover map for the year 2065	Land cover map for the year 2085	

## Results and discussion

### Hydrologic model calibration and validation

This study evaluated the sensitivity of input parameters in the SWAT model used for the modeling of average monthly flow-discharge. Out of 45 parameters, the 14 most sensitive ones given by the SWAT-CUP were calibrated using the following parameter identifiers:

- “v” means the existing parameter value is to be replaced.
- “a” means the existing parameter value is added to the existing parameter value.
- “r” means the existing parameter value is multiplied by (1 + a given value) (Abbaspour, 2015).

Sensitive parameters and ranges for hydrologic model are given in Table 2.

In the study, the 2001–2006 and 2008–2012 periods were selected as calibration and validation periods for the hydrologic model at a monthly scale. Since 2007 was a dry period and the riverbed was dry on many days, it was excluded from the calibration–validation process. The calculated goodness of fit test results (NSE) are given in Table 3 for both periods. The performance evaluation criteria (NSE) for watershed scale models proposed by Moriasi et al.

**Table 3** Calculated goodness of fit test results for calibration and validation processes

Statistics	Nash–Sutcliffe efficiency (NSE)
Calibration (2001–2006) Land Use (LU2006)	0.80
Validation (2008–2012) Land Use (LU2006)	0.89

(2007) were considered to evaluate model performance. Since both values were above 0.75, the model simulation were assumed to be “very good.” The calibration and validation results of the SWAT hydrological model are depicted in Fig. 2.

### Water quality model calibration and validation

In order to perform the sensitivity analysis as suggested by Abbaspour (2015), 500 simulations were run in a single iteration for the 12 water quality parameters, and 8 parameters with  $p < 0.05$  were considered sensitive. After the 5th iteration, the NSE performance statistic of the SWAT-CUP model was 0.84. List of sensitive water quality parameters and calibration results is given in Table 4.

ArcSWAT was run for the catchment with the same set of calibrated parameters for the calibration (2001–2006) and validation periods (2008–2012).

**Table 2** Sensitive parameters and ranges for hydrologic model

Hydrological parameters	Method	Min. value	Max. value
Initial SCS runoff curve number	r	36.60	59.79
Average slope length (m)	r	20.28	135.18
Lateral flow travel time (days)	a	13.66	13.66
Max. canopy storage (mm water)	a	17.40	17.40
Plant uptake compensation factor	r	0.84	0.84
Calibration coefficient for storage time constant	r	1.97	1.97
Time threshold used to define dormancy (hr)	a	9.06	9.06
Effective hydraulic conductivity in main channel alluvium (mm/hr)	a	4.29	4.29
Available water capacity of the soil layer (mm water/mm soil)	r	0.38	0.61
Saturated hydraulic conductivity (mm/hr)	r	0.14	0.69
Groundwater delay time (days)	r	57.33	57.33
Deep aquifer percolation fraction	r	0.24	0.24
Threshold depth of water in the shallow aquifer required for return flow to occur (mm water)	r	998.26	4991.31
Groundwater revap coefficient	r	0.12	0.12

**Fig. 2** Calibration and validation results of the SWAT hydrological model

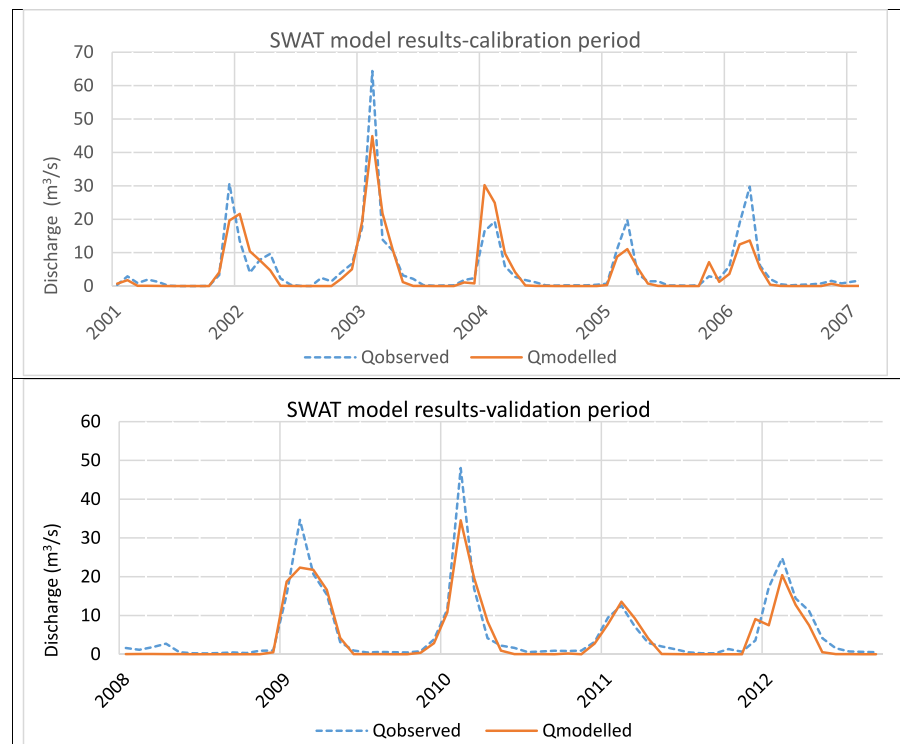


**Table 4** Calibration results for sensitive water quality parameters

Parameter	Method	Optimal value
Denitrification exponential rate coefficient	r	-0.98
Denitrification threshold water content	r	- 0.46
Fraction of porosity from which anions are excluded	r	0.87
Initial NO <sub>3</sub> concentration in the soil layer	a	81.23
Organic carbon content	a	0.03
Half-life of nitrate in the shallow aquifer	a	180.06
Initial depth of water in the shallow aquifer	r	55.49
Soluble nitrogen concentration in runoff	a	0.53

Simulated nitrate-nitrogen loads (in kilogram per month) are depicted in Fig. 3. The NSE value for the calibration period (2001–2006) were calculated as 0.77 and 0.69 for the verification period (2008–2012). The observed and modeled results shared certain similarities in their characteristics. However, there was a notable disparity, particularly in the peak values. This could be explained by the transport of nitrate from urban stormwater runoff to surface waters. Since there were no observations representing extreme precipitation on an

hourly basis, extreme events could not be examined in detail. On the other hand, since the NSE values were above 0.65, model simulations were assumed to be reliable for this study.

Using the best parameters, the SWAT model was run to simulate surface water nitrate levels in the basin. The model was run on a monthly time scale for reference (1985–2009) and future time periods under climate and land cover change scenarios. The NSE value was 0.69 for the modeling period of 1985–2009.



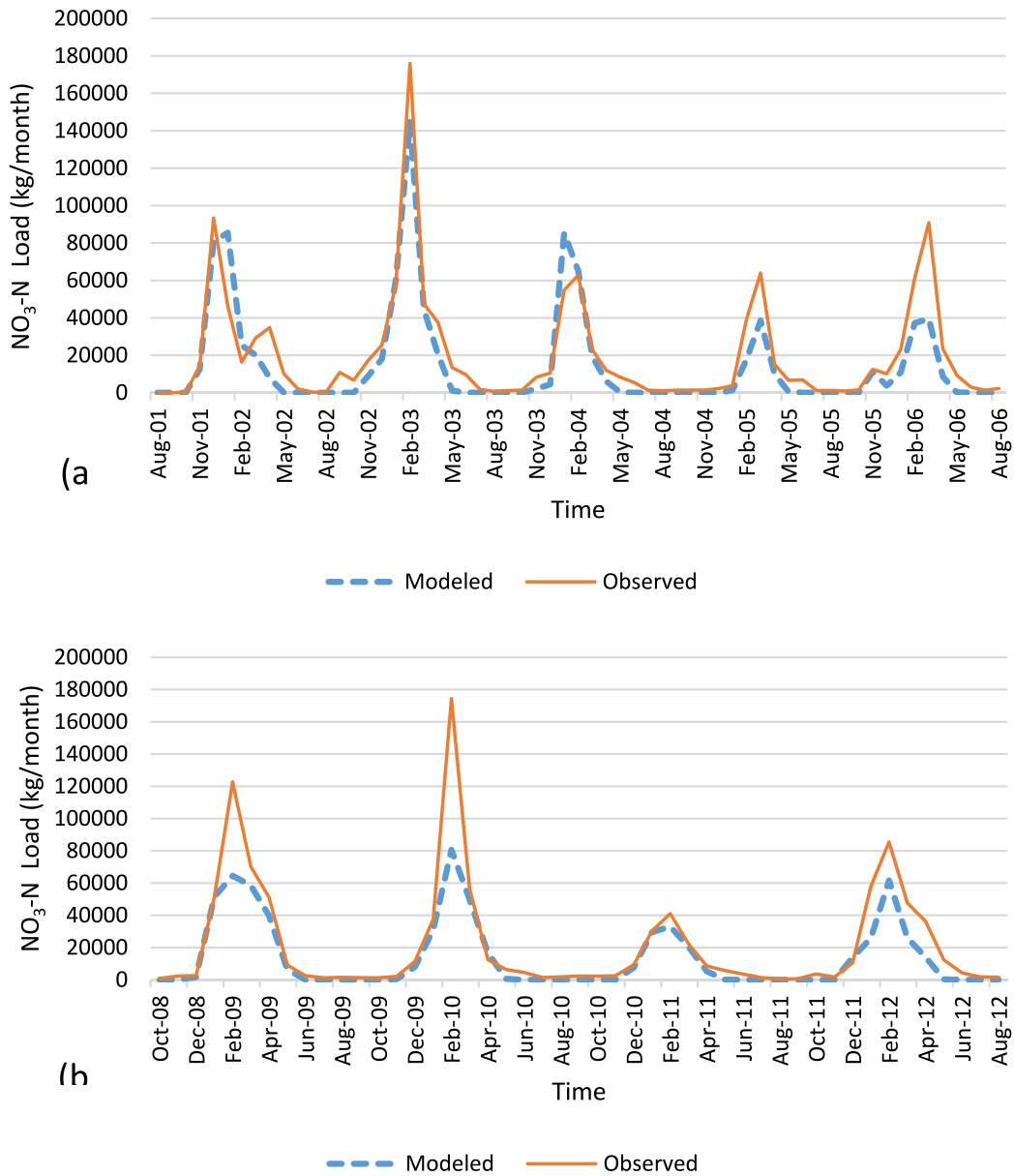


**Fig. 3** Observed and modeled  $NO_3-N$  loads of **a** calibration and **b** validation period

**Impact of climate change on nitrate transport**

The SWAT model was run for future period (2025–2100) climate conditions, and results revealed that surface water monthly average  $NO_3-N$  loads at the basin outlet decreased more than 50% in the mid-future (2050–2075), and 75% in the far-future (2075–2100) compared to the reference period (1985–2009) (Table 5). The reduction in nitrate

**Table 5** Relative change of the scenario period mean,  $NO_3$  loads, annual total precipitation, and discharge values at the basin outlet compared to the reference period (under climate change)

	2025–2050	2050–2075	2075–2100
$NO_3-N$ loads	–19.4	–52.4	–77.3
Annual total precipitation	–4.6	–10.9	–23.9
Discharge values	–19.1	–58.2	–90.4

transport from agricultural areas to the stream network could be explained by the decrease in rainfall (12% in 2050–2075, and 23% in the 2075–2100 period), accordingly, water discharge driven by climate change decreased by about 60% in the mid-future, and 90% in the far-future.

#### Impact of land cover change on nitrate transport

Keeping the reference period's climatic conditions constant, the SWAT model was run using the estimated land cover maps of future periods. The years 2035, 2065, and 2085 maps were used to model near-, mid-, and far-future periods. The objective was to examine the difference in transported nitrogen loads between reference and future periods under changing land cover conditions. Model results were compared to reference conditions that were represented by the 1990-CORINE land cover map and the 1985–2009 climate conditions. Results showed that, in contrast to climate change scenarios, surface water  $\text{NO}_3\text{-N}$  content showed an increasing trend at the basin outlet in the future period under the land cover change scenarios. The increase was 2.9% in 2025–2050, 3.9% in 2050–2075, and 5.5% in the 2075–2100 time period (see Table 6). Transitions in land cover classes played an important role in this increase. This was discussed in detail in the following sections of the paper.

#### The superposed impact of climate and land cover change on nitrate transport

When the superposed effects of climate and land cover changes at the basin outlet were evaluated, it was seen that the monthly average values of  $\text{NO}_3\text{-N}$  loads in the future period had decreased compared to the reference period. In the far-future, this reduction is expected to be about 70% (Table 6).

**Table 6** Percent change (%) in nitrate-nitrogen loads at the basin outlet compared to the reference period

Scenario	Near-future 2025–2050	Mid-future 2050–2075	Far-future 2075–2100
Climate change	–19.4	–52.4	–77.3
Land cover change	2.9	3.9	5.5
The combined impact of climate and land cover change	–10.9	–40.0	–71.3

The reduction in nitrate load in the future was explained by a decrease in the amount of nitrate transported to the surface water via less run-off and infiltration, which was driven by reduced rainfall. It could not be considered a positive effect of climate change on water quality. Furthermore, the transition from predominantly forestry to pastoral farming systems resulted in an increase in surface water nitrate loads, and the rate of this change was negligible compared to the impact of reduced rainfall. On the other hand, the combined impact of climate and land cover change was not equal to the sum of the individual effects of these two factors. Hence, there was a non-linear effect when these two factors were combined (see Table 6).

In summary, nitrate loads transported to surface water decreased by more than 75% in the far-future period under the climate change scenario (Table 6). This could be explained by a drastic decrease in rainfall patterns. This result stating “increasing temperature and decreasing rainfall will reduce nitrogen loading” was similar to the outcomes of previous studies (Shrestha et al., 2018 and Fan & Shibata, 2015). In contrast, land cover change increased transported nitrate loads by about 6% in the same period. The transition from predominantly forestry to pastoral farming systems resulted in an increase in surface water nitrate loads. Since the nitrogen loads (kg/ha year) transported to surface waters from pasture were higher compared to forest lands (USEPA, 1999), estimated transitions in land use in the study area decreased water quality under the land use scenario. The findings of the research confirmed previous studies (Jacobs et al., 2017; USEPA, 1999).

#### Spatial differentiation of surface water nitrate loads under scenarios

To represent the reference period climate and land cover conditions, the SWAT model was run using the CORINE 1990 land cover map and 1985–2009 period climate data. Model results showed that higher nitrate-nitrogen loads (up to 26,000 kg/month) were observed along the main channel and downstream of the river (Fig. 4a). In contrast, there was relatively less nitrate transport in the upstream sections. Lower nitrate loads at these sites could be explained by either lesser agricultural activity or specific land cover characteristics (Figure S1).

The model results investigating the impact of land cover change on water quality revealed that while there

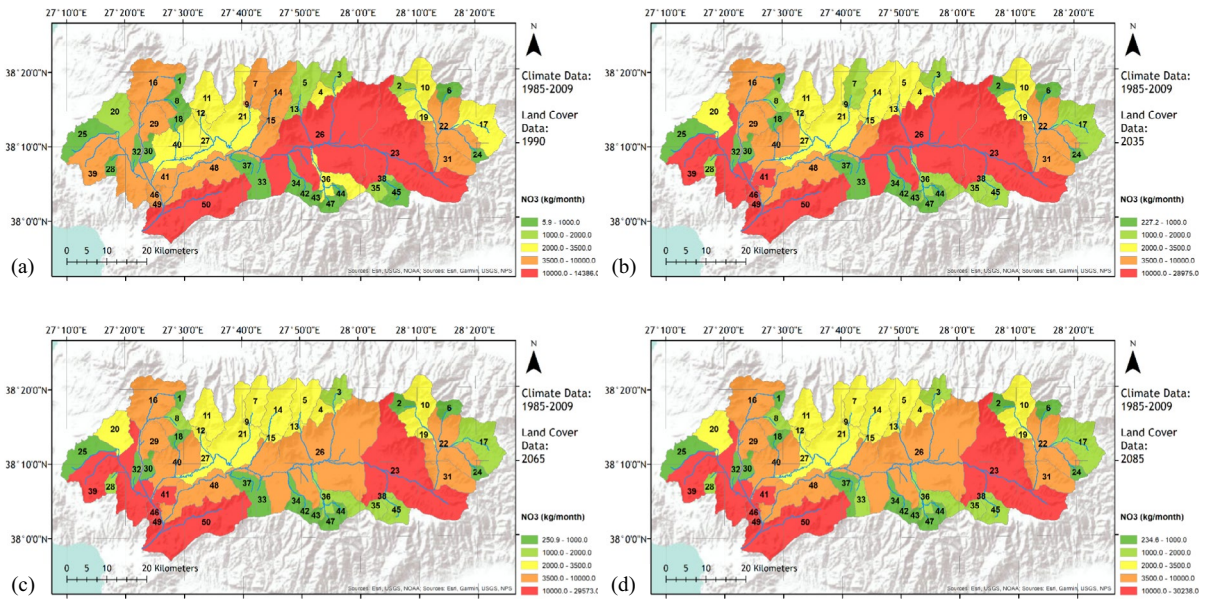


**Fig. 4** Surface water monthly average  $NO_3-N$  loads under **a** reference period, **b** land use change scenario (near-future period), **c** land use change scenario (mid-future period), **d** land use change scenario (far-future period)

was an increase in one region, there was a decrease in other locations. The distribution of  $NO_3-N$  loads at the sub-basin scale is depicted in Fig. 4b, c, and d. Since

the transitions in land cover classes were not distributed homogeneously, spatial differences were observed in the basin extent (Table S3). On the other hand, differentiation

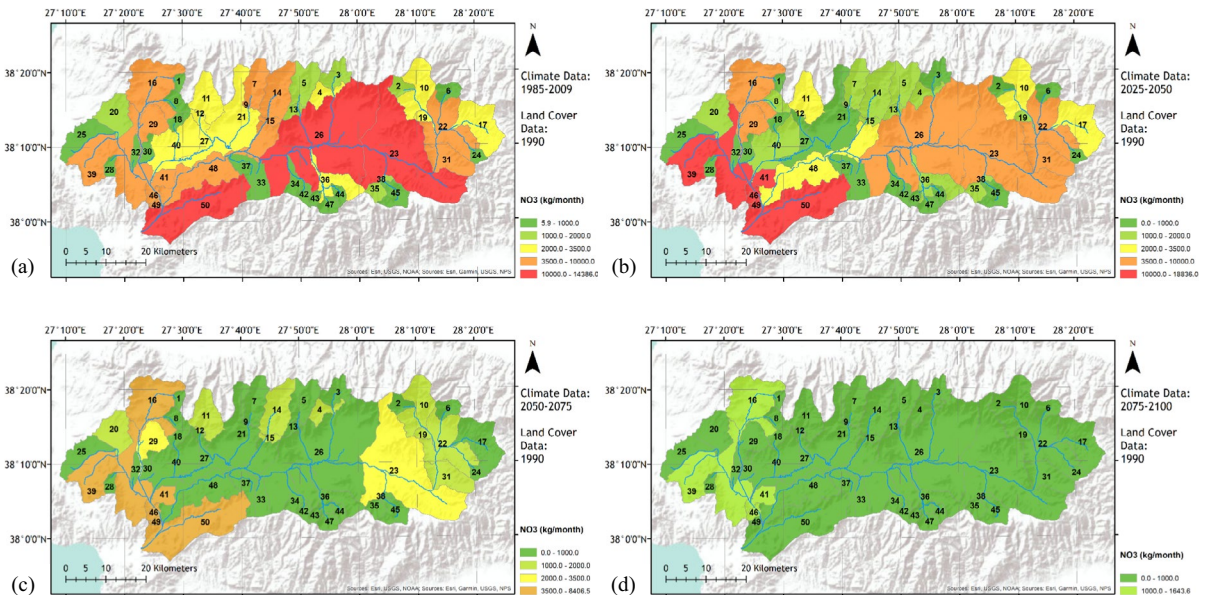


**Fig. 5** Surface water monthly average  $NO_3-N$  loads under **a** reference period, **b** climate change scenario (near-future period), **c** climate change scenario (mid-future period), **d** climate change scenario (far-future period)

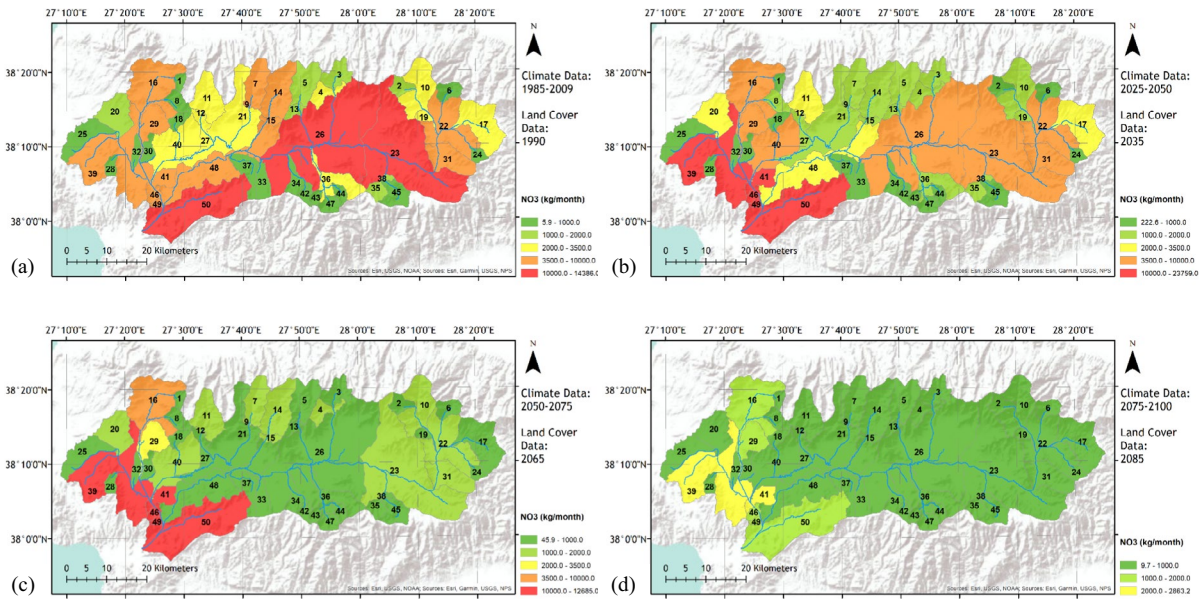


**Fig. 6** Surface water monthly average  $\text{NO}_3\text{-N}$  loads under **a** reference period (LC 1990), **b** climate and land use change scenarios (near-future period), **c** climate and land use change

scenarios (mid-future period), **d** climate and land use change scenarios (far-future period)

is also caused by spatial heterogeneity in soil properties (e.g., available water capacity, silt content). As has been presented in Table S3, most of the change (spatially) in the land cover class transitions between the reference and scenario periods was from forest to pasture. The nitrate loads transported into surface waters from different land cover types were evaluated to assess model outputs. Since the nitrogen loads (kg/ha year) transported to surface waters from pasture were higher compared to forest lands (Table S4 and Table S5), transitions from forests to pasture/agricultural/grassland areas have a negative impact on water quality.

The model results investigating the impact of climate change on water quality in each sub-basin showed that there were decreases in nitrate loads in almost all sub-basins over time (Fig. 5). This result could not be considered a positive effect of climate change on water quality. The reduction was explained by a decrease in the amount of nitrate transported to the surface water via less run-off and infiltration, which was driven by reduced rainfall.

Under the superposed scenario (combined impact of climate and land use change), the spatial distribution and amount of nitrate loads in each sub-basin were evaluated. Results revealed that, despite the negative impact of land cover change scenarios that increased nitrate loads transported to the surface,

the total amount of nitrate loads was comparatively low in the future period. As was explained previously, the reduction was explained by a decrease in the amount of nitrate transported to the surface water via less run-off and infiltration which was driven by reduced rainfall (Fig. 6).

In summary, besides the temporal differences, spatial variations in nitrate loads were also significant in the region, and this should be considered by decision-makers when developing management plans. Priority in the development process of pollution mitigation plans could be given to sites with higher transported nitrogen loads.

### Conclusions

The novel contribution of the study was to investigate the individual and combined impacts of climate and land cover change on water quality with high spatial and temporal resolution. The study results revealed that the simulation accuracy of nitrogen loading was lower than that of runoff. Since observation of nitrogen loading in the basin was less frequent compared to discharge, water quality simulation was less accurate. Furthermore, decreasing the intensity of precipitation

could result in great reductions in nitrate transport to surface water under the climate change scenario. A decreased nitrate load in the future could not be considered a positive effect of climate change on water quality. The reduction was explained by a decrease in the amount of nitrate transported to the surface water via less run-off and infiltration, which was driven by reduced rainfall. Furthermore, the transition from predominantly forestry to pastoral farming systems resulted in an increase in surface water nitrate loads. However, the rate of this change was negligible compared to the impact of reduced rainfall. Moreover, the superposed impact of climate and land cover change was not equal to the sum of the individual effects of these two factors. Hence, there was a non-linear effect when these two factors were combined.

In summary, it can be concluded that prediction of land use changes based on LCM and attribution of changes in water quality to land use changes using the SWAT model can be of great use to environmental managers.

**Acknowledgements** We thank the project team members who provided insight and expertise that greatly assisted the research.

**Author contribution** Hulya Boyacioglu was responsible for:

- Conception and design of the work.
- Data collection.
- SWAT model calibration validation.
- Data analysis and interpretation.
- Writing the article.

Mert Can Gunacti, Filiz Barbaros, Ali Gul, and Gulay Onuslu Gul were responsible for:

- Data collection.
- Model input preparation.
- SWAT model calibration validation.
- Writing the article.

Tugba Ozturk and M. Levent Kurnaz were responsible for:

- Climate modeling.

**Funding** This research was supported by the 1003 Programme of the Scientific and Technological Research Council of Turkey (TUBITAK) under Grant Agreement No 116Y423.

**Data availability** All relevant data are included in the paper or its Supplementary Information.

**Declarations**

**Competing interests** The authors declare no competing interests.

**Conflict of interest** The authors declare there is no conflict.

## References

- Abbaspour, K. C. (2015) SWAT-calibration and uncertainty programs (CUP)—A user manual. *Swiss Federal Institute of Aquatic Science and Technology, Eawag, Duebendorf*, 1–100.
- Agacayak, T., Kindap, T., Unal, A., Pozzoli, L., Mallet, M., & Solmon, F. (2015). A case study for Saharan dust transport over Turkey via RegCM4.1 model. *Atmospheric Research*, *153*, 392–403. <https://doi.org/10.1016/j.atmosres.2014.09.012>
- Amiri, S. N., Khoshravesh, M., & Valashedi, R. N. (2023). Assessing the effect of climate and land use changes on the hydrologic regimes in the upstream of Tajan river basin using SWAT model. *Applied Water Science*, *13*, 130. <https://doi.org/10.1007/s13201-023-01932-3>
- Anand, J., Gosain, A. K., & Khosa, R. (2018). Prediction of land use changes based on land change modeler and attribution of changes in the water balance of Ganga basin to land use change using the SWAT model. *Science of the Total Environment*, *644*, 503–519.
- Ansari, A., & Golabi, M. H. (2019). Using ecosystem service modeler (esm) for ecological quality, rarity and risk assessment of the wild goat habitat, in the Haftad-Gholleh protected area. *International Soil and Water Conservation Research*, *7*(4), 346–353. <https://doi.org/10.1016/j.iswcr.2019.08.004>
- Arnold, J. G., Kiniry, J. R., Srinivasan, R., Williams, J. R., Haney, E. B., & Neitsch, S. L. (2012). *Soil and water assessment tool. Input/output documentation Version 2012*. Texas Water Resource Institute. TR-439.
- Bai, Y., Ochuodho, T. O., & Yang, J. (2019). Impact of land use and climate change on water-related ecosystem services in Kentucky, USA. *Ecological Indicators*, *102*, 51–64. <https://doi.org/10.1016/j.ecolind.2019.01.079>
- Choi, J., Park, B., Kim, J., Lee, S., Ryu, J., Kim, K., & Kim, Y. (2021). Determination of NPS pollutant unit loads from different land uses. *Sustainability*, *13*. <https://doi.org/10.3390/su13137193>
- Delia, K. A., Haney, C. R., Dyer, J. L., & Paul, V. G. (2021). Spatial analysis of a Chesapeake Bay Sub-Watershed: How land use and precipitation patterns impact water quality in the James River. *Water*, *13*(11), 1592. <https://doi.org/10.3390/w13111592>
- Demiroglu, O. C., Turp, M., Ozturk, T., & Kurnaz, M. L. (2015). Impact of climate change on ski resorts in the Balkans, the Middle East and the Caucasus: A preliminary assessment for ski tourism in Northeast Turkey. In *Proceedings of the 4th International Conference on Climate, Tourism and Recreation CCTR 2015*.
- EarthExplorer, (2019) U.S. Geological Survey. <https://earthexplorer.usgs.gov/> (accessed 13 March 2022).
- Fan, M., & Shibata, H. (2015). Simulation of watershed hydrology and stream water quality under land use and climate change scenarios in Teshio River watershed, northern Japan. *Ecological Indicators*, *50*, 79–89. <https://doi.org/10.1016/j.ecolind.2014.11.003>
- Gashaw, T., Tulu, T., Argaw, M., & Worqlul, A. W. (2018). Modeling the hydrological impacts of land use/land cover changes in the Andassa watershed, Blue Nile Basin

- Ethiopia. *Science of the Total Environment*, 619–620, 1394–1408. <https://doi.org/10.1016/j.scitotenv.2017.11.191>
- Gunacti, M. C., Kandemir, F. A., Najar, M., Kuzucu, A., Uyar, M., Barbaros, F., Boyacioglu, H., Gul, G. O., & Gul, A. (2022). Attribution of changes in water balance of a basin to land-use changes through combined modelling of basin hydrology and land-use dynamics. *Journal of Water and Climate Change*, 13(11), 4087–4104.
- Hashim, B. M., Al Maliki, A., Sultan, M. A., et al. (2022). Effect of land use land cover changes on land surface temperature during 1984–2020: A case study of Baghdad city using landsat image. *Natural Hazards*, 112, 1223–1246. <https://doi.org/10.1007/s11069-022-05224-y>
- Hosseini, M., Geissen, V., González-Pelayo, O., Serpa, D., Machado, A. I., Ritsema, C., & Keizer, J. J. (2017). Effects of fire occurrence and recurrence on nitrogen and phosphorus losses by overland flow in maritime pine plantations in north-central Portugal. *Geoderma*, 289, 97–106. <https://doi.org/10.1016/j.geoderma.2016.11.033>
- Jacobs, S. R., Breuer, L., Butterbach-Bahl, K., Pelster, D. E., & Rufino, M. C. (2017). Land use affects total dissolved nitrogen and nitrate concentrations in tropical montane streams in Kenya. *Science of the Total Environment*, 603, 519–532. <https://doi.org/10.1016/j.scitotenv.2017.06.100>
- Khadka, D., Babel, M. S., & Kamalamma, A. G. (2023). Assessing the impact of climate and land-use changes on the hydrologic cycle using the SWAT model in the Mun River Basin in Northeast Thailand. *Water*, 15(20), 3672. <https://doi.org/10.3390/w15203672>
- Khoi, D. D., & Murayama, Y. (2010). Forecasting areas vulnerable to forest conversion in the Tam Dao National Park Region Vietnam. *Remote Sensing*, 2(5), 1249–1272. <https://doi.org/10.3390/rs2051249>
- Kiehl, J. T., Hack, J. J., Bonan, G. B., Boville, B. A., Breigleb, B. P., Williamson, D. L., & Rasch, P. J. (1996). *Description of the NCAR Community Climate Model (CCM3)*, (No. NCAR/TN-420+STR). University Corporation for Atmospheric Research. <https://doi.org/10.5065/D6FF3Q99>
- Kim, D.-H., Sexton, J. O., Noojoody, P., Huang, J., Anand, A., Channan, S., Feng, M., & Townshend, J. R. (2014). Global, Landsat-based forest-cover change from 1990 to 2000. *Remote Sensing of Environment*, 155, 178–193. <https://doi.org/10.1016/j.rse.2014.08.017>
- Koulov B & Zhelezov G. (2016). *Sustainable mountain regions: Challenges and perspectives in Southeastern Europe*. <https://doi.org/10.1007/978-3-319-27905-3>. Publisher Springer Cha
- Mahmoodi, N., Wagner, P. D., Kiesel, J., & Fohrer, N. (2021). Modeling the impact of climate change on streamflow and major hydrological components of an Iranian Wadi system. *Journal of Water and Climate Change*, 12(5), 1598–1613. <https://doi.org/10.2166/wcc.2020.098>
- Mehdi, B., Lehner, B., Gombault, C., Michaud, A., Beaudin, I., Sottile, M.-F., & Blondlot, A. (2015). Simulated impacts of climate change and agricultural land use change on surface water quality with and without adaptation management strategies. *Agriculture, Ecosystems & Environment*, 213, 47–60. <https://doi.org/10.1016/j.agee.2015.07.019>
- Mekonnen, Y. A., & Manderso, T. M. (2023). Land use/land cover change impact on streamflow using Arc-SWAT model, in case of Fetam watershed, Abbay Basin. *Ethiopia. Appl Water Sci*, 13, 111. <https://doi.org/10.1007/s13201-023-01914-5>
- MoAF. (2019). *Kiçik Menderes River Basin Management Plan Final Report*. Ministry of Agriculture and Forestry-MoAF, General Directorate of Water Management. Republic of Turkey Ankara.
- Moriasi, D., Arnold, J., Van Liew, M., Bingner, R., Harmel, R., & Veith, T. (2007). Model evaluation guidelines for systematic quantification of accuracy in watershed simulations. *Transactions of the ASABE*, 50(3), 885–900. <https://doi.org/10.13031/2013.23153>
- Mustafa, A. M., & Szydlowski, M. (2020). The impact of spatiotemporal changes in land development (1984–2019) on the increase in the runoff coefficient in Erbil. *Kurdistan Region of Iraq. Remote Sens.*, 12(8), 1302. <https://doi.org/10.3390/rs12081302>
- Mustafa, A. M., Muhammed, H. H., & Szydlowski, M. (2019). Extreme rainfalls as a cause of urban flash floods; a case study of the Erbil-Kurdistan Region of Iraq. *Acta Scientiarum Polonorum. Formatio Circumiectus*, 18(3), 113–132. <https://doi.org/10.15576/ASP.FC/2019.18.3.113>
- Oğuz, K., & Akin, B. S. (2018). Evaluation of temperature, precipitation and dust aerosol simulations for Turkey. *International Journal of Current Research*, 10(09), 73225–73233. <https://doi.org/10.24941/ijcr.32322.09.2018>
- Ozturk, T. (2023). Projected future changes in extreme climate indices over Central Asia Using RegCM4.3.5. *Atmosphere*, 2023(14), 939. <https://doi.org/10.3390/atmos14060939>
- Ozturk, T., Turp, M. T., Türkeş, M., & Kurnaz, M. L. (2018). Future projections of temperature and precipitation climatology for CORDEX-MENA domain using RegCM4. 4. *Atmospheric Research*, 206, 87–107.
- Rostami, S., He, J., & Hassan, Q. K. (2018). Riverine water quality response to precipitation and its change. *Environments*, 5(1), 8. <https://doi.org/10.3390/environments5010008>
- Saha, S., et al. (2014). The NCEP Climate Forecast System Version 2. *Journal of Climate*, 27, 2185–2208. <https://doi.org/10.1175/JCLI-D-12-00823.1>
- Serpa, D., Nunes, J. P., Keizer, J. J., & Abrantes, N. (2017). Impacts of climate and land use changes on the water quality of a small Mediterranean catchment with intensive viticulture. *Environmental Pollution*, 224, 454–465. <https://doi.org/10.1016/j.envpol.2017.02.026>
- Sholichin, M., & Prayogo, T. B. (2021). Assessment of the impact of land cover type on the water quality in lake Tondano using a SWAT model. *Journal of Southwest Jiaotong University*, 56(1). <https://doi.org/10.35741/issn.0258-2724.56.1.25>
- Shrestha, S., Bhatta, B., Shrestha, M., & Shrestha, P. K. (2018). Integrated assessment of the climate and landuse change impact on hydrology and water quality in the Songkhram River Basin, Thailand. *Science of the Total Environment*, 643, 1610–1622. <https://doi.org/10.1016/j.scitotenv.2018.06.306>
- Soilgrids, (2019). International Soil Reference and Information Center (ISRIC). World Soil Information. [https://soilrids.org/#/?layer=ORCDRC\\_M\\_sl2\\_250m&vector=1](https://soilrids.org/#/?layer=ORCDRC_M_sl2_250m&vector=1) (accessed 01 November 2019).

- Solaimani, K., Shokrian, F., & Darvishi, S. (2023). An assessment of the integrated multi-criteria and new models efficiency in watershed flood mapping. *Water Resour Manage*, 37, 403–425. <https://doi.org/10.1007/s11269-022-03380-1>
- Szpakowski, W., & Szydłowski, M. (2018). Probable rainfall in Gdańsk in view of climate change. *Acta Scientiarum Polonorum Formatio Circumiectus*, 17(3), 175–183. <https://doi.org/10.15576/ASP.FC/2018.17.3.175>
- Tu, J. V. (1996). Advantages and disadvantages of using artificial neural networks versus logistic regression for predicting medical outcomes. *Journal of Clinical Epidemiology*, 49(11), 1225–1231. [https://doi.org/10.1016/S0895-4356\(96\)00002-9](https://doi.org/10.1016/S0895-4356(96)00002-9)
- TURKSTAT. (2023). Turkish Statistical Institute-TURKSTAT, 2022 Turkish population census results.
- USEPA. (1999). *Protocol for developing nutrient TMDL's, United States Environmental Protection Agency-USEPA, EPA 841-B-99-007*. Office of Water (4503F), Washington, DC.
- Whitehead, P. G., Wilby, R. L., Battarbee, R. W., Kernan, M., & Wade, A. J. (2009). A review of the potential impacts of climate change on surface water quality. *Hydrological Sciences Journal*, 54(1), 101–123. <https://doi.org/10.1623/hysj.54.1.101>
- Yang, X., Warren, R., He, Y., Ye, J., Li, Q., & Wang, G. (2018). Impacts of climate change on tn load and its control in a river basin with complex pollution sources. *Science of the Total Environment*, 615, 1155–1163. <https://doi.org/10.1016/j.scitotenv.2017.09.288>
- Yariyan, P., Avand, M., Abbaspour, R. A., Torabi Haghghi, A., Costache, R., Ghorbanzadeh, O., Janizadeh, S., & Blaschke, T. (2020). Flood susceptibility mapping using an improved analytic network process with statistical models. *Geomatics, Natural Hazards and Risk*, 11(1), 2282–2314. <https://doi.org/10.1080/19475705.2020.1836036>
- Zango, B. S., Seidou, O., Sartaj, M., Nakhaei, N., & Stiles, K. (2022). Impacts of urbanization and climate change on water quantity and quality in the Carp River watershed. *Journal of Water and Climate Change*, 13(786), 816. <https://doi.org/10.2166/wcc.2021.158>
- Zhu, X., Chang, K., Cai, W., Zhang, A., Yue, G., & Zhao, X. (2022). Response of runoff and nitrogen loadings to climate and land use changes in the middle Fenhe River basin in Northern China. *Journal of Water and Climate Change*, 13(7), 2817–2836. <https://doi.org/10.2166/wcc.2022.121>

**Publisher's Note** Springer Nature remains neutral with regard to jurisdictional claims in published maps and institutional affiliations.

Springer Nature or its licensor (e.g. a society or other partner) holds exclusive rights to this article under a publishing agreement with the author(s) or other rightsholder(s); author self-archiving of the accepted manuscript version of this article is solely governed by the terms of such publishing agreement and applicable law.